

**Supporting Information for**

**Manuscript ID.: CE-ART-07-2010-000472**

**Uniform ZnSe Microspheres Self-Assembled from ZnSe Polyhedron Shaped Nanocrystals**

Na Wang, Rujia Zou, Huihui Chen, Haihua Chen, Yangang Sun, Jianghong Wu, Qiwei Tian, Jianmao Yang, Zhigang Chen, and Junqing Hu<sup>\*</sup>

State Key Laboratory for Modification of Chemical Fibers and Polymer Materials,  
College of Materials Science and Engineering, Donghua University, Shanghai 201620,  
China

Electronic mail: [hu.junqing@dhu.edu.cn](mailto:hu.junqing@dhu.edu.cn)

The synthetic process produces a large quantity of gaseous H<sub>2</sub>O and a considerable quantity of N<sub>2</sub> and H<sub>2</sub>. To minimizing the risk of high overpressure inside the autoclave, 75% of the maximum capacity of the autoclave was employed safely in our experiment. Also, other volumes (e.g., 50% and 60% of the maximum capacity of the autoclave) were tried. The SEM images of the products are shown in Figure S1 (a) and (b), respectively. When 50% or 60% of the maximum capacity of the autoclave used was employed in our experiment, most of the products display irregular shape, and only a small amount of them are microspheres; all of the diffraction peaks in the XRD patterns (two insets in them) from the two samples, respectively, can be indexed as those from the known blend-structured (cube) ZnSe.

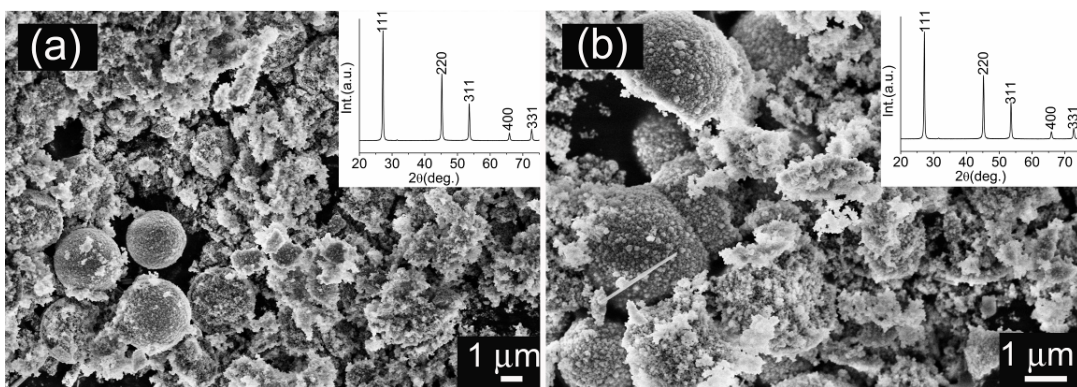


Figure S1. SEM images of the ZnSe products prepared under (a) 50% (sample 14) and (b) 60% (sample 15) of the capacity of the autoclave used, respectively, insets showing the corresponding XRD patterns, respectively.

The XRD patterns of the ZnSe solid microspheres synthesized at different reaction times are shown in Figure S2 (a) (sample 3, 12 h), (b) (sample 6, 2 h), and (c) (sample 8, 6 h), respectively, and the XRD pattern of the ZnSe hollow microspheres is shown in Figure S2 (d) (sample 12). Both of the XRD patterns of these ZnSe solid microspheres, Figure S2 (a), and hollow microspheres, and Figure S2 (d), can be indexed as those from the cubic ZnSe; no characteristic peaks due to the source materials and other impurities are detected. However, when the reaction time is 2 h, besides the strong peaks from the ZnSe (main phase), it is also observed that some weak peaks due to Se and ZnO (as-formed impurities) are detected, shown in Figure S2 (b). When the reaction time is prolonged to 4 h, it is clear that the peaks due to the impurities (Se and ZnO) become weaker than those obtained at 2 h, suggesting the contents of the impurities are less than those obtained at 2 h, Figure S2 (c). So, based on the above results, to conclude, a longer reaction time, e.g., 12 h, could be beneficial to obtain pure ZnSe products.

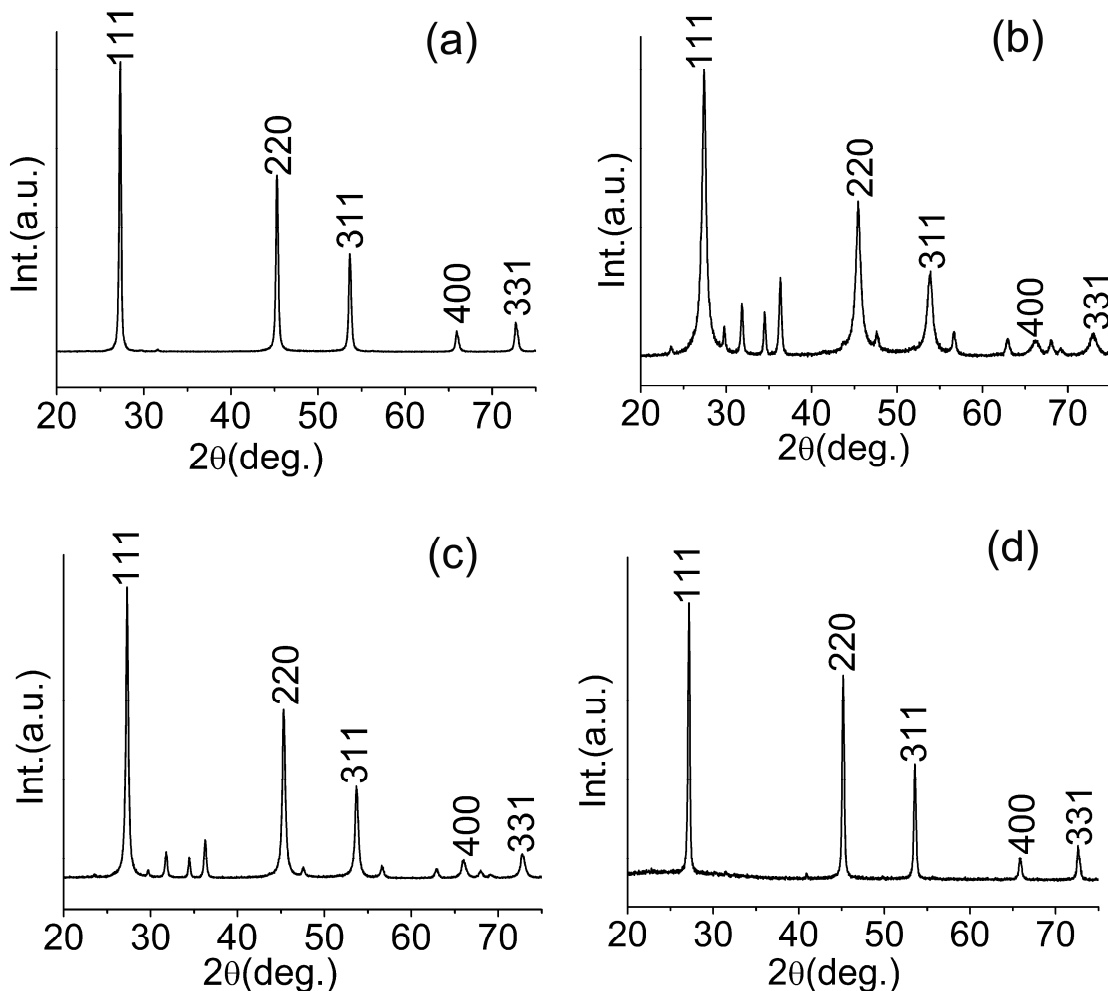


Figure S2. XRD patterns of the products using  $\text{SeO}_2$  as Se source and at  $180^\circ\text{C}$  via different reaction times: (a) 12 h (sample 3), (b) 2 h (sample 6), (c) 6 h (sample 8) and (d) oleyl amine works as surfactant, 12 h (sample 12).

In our experiments, Se powders and  $\text{SeO}_2$  was used as Se source, respectively. Using Se powders as a source, Se powders can not dissolve in water, but easily dissolve in strong base solution, producing  $\text{Se}^{2-}$  in the base solution ( $3\text{Se} + 6\text{OH}^- \leftrightarrow 2\text{Se}^{2-} + \text{SeO}_3^{2-} + 3\text{H}_2\text{O}$ ). In this process, the obtained  $\text{Se}^{2-}$  ions react with  $\text{Zn}^{2+}$ , forming primary  $\text{ZnSe}$  nanocrystals which show irregular shape, then hydrazine was injected into the solution to

reduce the  $\text{SeO}_3^{2-}$  ions into Se ( $3\text{SeO}_3^{2-} + 3\text{N}_2\text{H}_4 \rightarrow 3\text{Se} + 3\text{N}_2\uparrow + 3\text{H}_2\text{O} + 6\text{OH}^-$ ), in which as-formed Se was disproportionated in the alkaline solution to generate  $\text{Se}^{2-}$  ions again ( $3\text{Se} + 6\text{OH}^- \leftrightarrow 2\text{Se}^{2-} + \text{SeO}_3^{2-} + 3\text{H}_2\text{O}$ ). These  $\text{Se}^{2-}$  ions react with  $\text{Zn}^{2+}$ , forming ZnSe nanocrystals, and as-formed ZnSe nanocrystals would be deposited on the surface of the primary ZnSe nanocrystals and irregular shaped ZnSe products are obtained, as shown in Figure S3 (a). However, Using  $\text{SeO}_2$  as a source,  $\text{SeO}_2$  is a good solute in both water and base solution ( $\text{SeO}_2 + \text{H}_2\text{O} \rightarrow \text{H}_2\text{SeO}_3$ ;  $\text{H}_2\text{SeO}_3 + 2\text{NaOH} \rightarrow \text{Na}_2\text{SeO}_3 + 2\text{H}_2\text{O}$ ). In this process, the generated  $\text{Se}^{2-}$  ions will only be produced after hydrazine was injected into the solution. At this time, the  $\text{Se}^{2-}$  ions and  $\text{Zn}^{2+}$  in the solution are saturated, and ZnSe microspheres made of ZnSe faceted nanocrystals formed, as shown in Figure S3 (b).

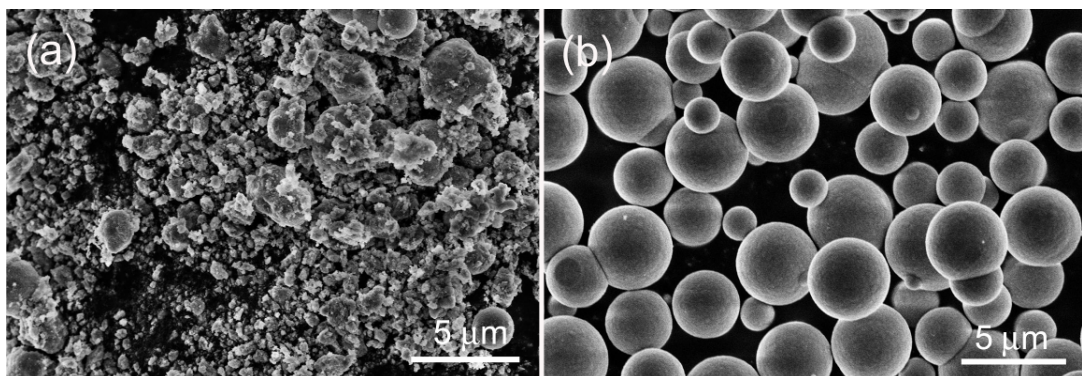


Figure S3. SEM images of the ZnSe microspheres prepared at 180 °C and 0.5 h with different Se source: (a) Se (sample 13), (b)  $\text{SeO}_2$  (sample 4).

The Ostwald ripening mechanism may also affect the formation of these ZnSe hollow microspheres through the present hydrothermal treatment. During this process, the nanocrystals located in the central part of the initial colloids are smaller or less dense than

those from the outer parts, as shown in Fig. 6 (d) or in Figure S4. Through the Ostwald-ripening process, the growth of those large crystals from the outer part is believed to be faster and easier than that of those in the central which have a higher solubility, and thus the nanocrystals in the central of the microspheres dissolve and hollow microspheres are prepared.<sup>1-3</sup> However, in contrast to the well described “hard-template” processes for the hollow microspheres,<sup>4</sup> the detailed growth mechanisms of the hollow ZnSe microspheres in the present study, are not fully understood, and require more systematic examination.

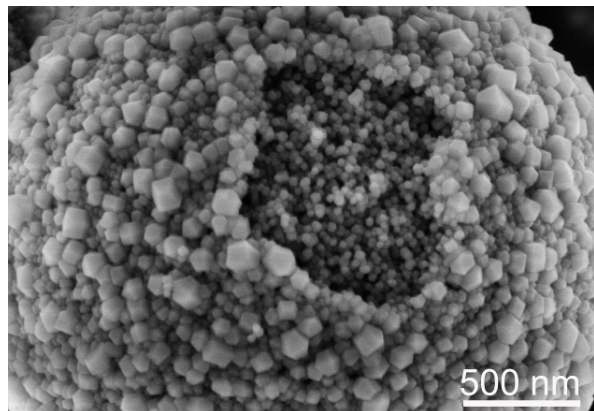


Figure S4. The high-magnification SEM image of the ZnSe microspheres prepared at 180 °C and 12 h (sample 3).

## Reference

- 1 Q. Zhang, W. S. Wang, J. Goebel and Y. D. Yin, *Nano Today*, 2009, **4**, 497.
- 2 X. F. Sun, S. G. Wang, X. M. Zhang, J. P. Chen, X. M. Li, B. Y. Gao and Y. Ma, *J. Colloid Interf. Sci.*, 2009, **335**, 11.
- 3 X. W. Lou, L. A. Archer and Z. C. Yang, *Adv. Mater.*, 2008, **20**, 3987.

4 (a) X. L. Xu and S. A. Asher, *J. Am. Chem. Soc.*, 2004, **126**, 7940; (b) G. J. Guan, Z. P. Zhang, Z. Y. Wang, B. H. Liu, D. M. Gao and C. G. Xie, *Adv. Mater.*, 2007, **19**, 2370.